Investigation of Web Hole Effects on Capacities of Cold-formed Steel Channel Members

Ngoc Hieu Pham[1]

[1] Faculty of Civil Engineering, Hanoi Architectural University, Hanoi, Vietnam
hieupn@hau.edu.vn

Abstract. Cold-formed steel structures have been widely applied in structural buildings with advantages in manufacturing, transportation and assembly. Holes can be pre-punched in the sectional members to allow technical pipes to go throughout such as electricity, water or ventilation. This affects the capacities of these such members which have been considered in the design standards in America or Australia/New Zealand. The paper, therefore, investigates the effects of web holes on the capacities of cold-formed steel channel members under compression or bending. Their capacities can be determined according to the American Specification AISI S100-16. The investigated results are the base for analysing the effects of web hole dimensions on the behaviors and capacities of cold-formed steel channel members. It was found that the capacity reductions were obtained for compressive members with the increase in hole sizes, but the flexural capacities were noticeable increase with the increase in the hole heights.

Keywords: Effects, Capacities, Web Holes, Cold-formed Steel Channel Members.

1 Introduction

Cold-formed steel members have been progressively applied in structural buildings due to their advantages compared to traditional steel structures [1]. Channel sections are the common products worldwide for many decades [2]. Holes are pre-punched in the webs of such members to allow the technical pipes such as water and electricity to go throughout with the variation of hole shapes. The presence of holes has been demonstrated to reduce the capacities of these cold-formed steel members and has been considered in the American and Australian/New Zealand design standards ([3], [4]). According to these standards, a new method has been introduced in the design of cold-formed steel members namely the Direct Strength Method (DSM) which has been illustrated to be innovative compared to the traditional design method – the Effective Width Method [5]. The DSM will be used for the investigation in this paper.

The DSM allows the designer to directly predict the capacities of cold-formed steel members based on the determination of elastic buckling loads. These buckling loads can be provided by utilising several software programs for buckling analysis of cold-formed steel sections such as CUFSM [6] or THIN-WALL-2 [7]. The application of

these software programs in the design is reported in the works of Pham [8] or Pham and Vu [9]. For cold-formed steel sections with perforations, the determination of elastic buckling loads was studied and subsequently proposed by Moen and Schafer ([10], [11], [12], [13], [14], [15], [16]). Their research results were the base for the development of a module software program CUFSM funded by the American Iron and Steel Institute ([17], [18]). This module software program will be introduced and applied in the buckling analysis of cold-formed steel sections with perforations in this paper.

The paper presents the application of the DSM in the determination of capacities of cold-formed steel channel members with perforations according to the American Specification AISI S100-16 [3]. The rectangular hole shapes are considered and are arranged evenly with the variation of the hole sizes. The hole heights vary from 0.2 to 0.8 times of the investigated sectional depths whereas their lengths are from 0.5 to 2.0 times of the depths. The material properties are regulated in the American Specification [3]. The boundary conditions are varied to obtain different buckling modes of the investigated cold-formed steel members under compression or bending. The investigated results will be used to analyse the influence of hole sizes on the capacities of cold-formed steel channel members with perforations under compression or bending.

2 Determination of Capacities of Cold-formed Steel Members under Compression or Bending According to The American Specification AISI S100-16

The provisions for the design of cold-formed steel members are presented in Chapter E for compression and Chapter F for bending according to the American Specification AISI S100-16 [3]. The DSM for the design of cold-formed steel members is presented in this paper.

2.1 Member in Compression

The nominal axial strength (P_n) is the least of three following strength values including global buckling strength (P_{ne}), local buckling strength (P_{nl}), and distortional buckling strength (P_{nd})

Global buckling strength (P_{ne})

$$P_{ne} = \left(0.658^{\lambda_c^2} \right) P_y \qquad \text{if } \lambda_C \leq 1.5 \qquad (1)$$

$$P_{ne} = \left(\frac{0.877}{\lambda_c^2} \right) P_y \qquad \text{if } \lambda_C > 1.5 \qquad (2)$$

where $\lambda_c = \sqrt{P_y / P_{cre}}$;

P_y is the yield strength of the gross section;

P_{cre} is the elastic global buckling strength, is taken as the smaller of the following values:

$$P_{ey} = \frac{\pi^2 EI_y}{(K_y L)^2} \tag{3}$$

$$P_{exz} = \frac{1}{2\beta}\left[(P_{ex} + P_t) - \sqrt{(P_{ex} + P_t)^2 - 4\beta P_{ex} P_t}\right] \tag{4}$$

$$P_{ex} = \frac{\pi^2 EI_x}{(K_x L)^2};\ P_t = \frac{1}{r_o^2}\left(GJ + \frac{\pi^2 EC_w}{(K_t L)^2}\right);\ r_o = \sqrt{x_o^2 + y_o^2 + \frac{I_x + I_y}{A_g}};$$

The sectional properties (I_x, I_y, J, A_g, x_o, y_o, r_o) are determined on the basis of the gross-section. These properties for perforated sections can be determined using the "weighted average" approach as presented in Table 2.3.2-1 of the specification [3] based on the ratio between the segment length of the gross-section and the net section, as follows:

$$I_{avg} = \frac{I_g L_g + I_{net} L_{net}}{L};\ J_{avg} = \frac{J_g L_g + J_{net} L_{net}}{L};$$

$$r_{o,avg} = \sqrt{x_{o,avg}^2 + y_{o,avg}^2 + \frac{I_{x,avg} + I_{y,avg}}{A_{avg}}};\ A_{avg} = \frac{A_g L_g + A_{net} L_{net}}{L};$$

$$x_{o,avg} = \frac{x_{o,g} L_g + x_{o,net} L_{net}}{L};\ y_{o,avg} = \frac{y_{o,g} L_g + y_{o,net} L_{net}}{L};$$

$C_{w,net}$ is the net warping constant assuming the hole height h_{hole*} as determined in Eq.(5), where h_{hole} is the actual hole height and D is the sectional depth

$$h_{hole*} = h_{hole} + \frac{1}{2}(H - h_{hole})\left(\frac{h_{hole}}{H}\right)^{0,2} \tag{5}$$

Local buckling strength (P_{nl})

$$P_{nl} = \begin{cases} P_{ne} & for\ \lambda_l \le 0.776 \\ \left[1 - 0.15\left(\frac{P_{crl}}{P_{ne}}\right)^{0.4}\right]\left(\frac{P_{crl}}{P_{ne}}\right)^{0.4} P_y & for\ \lambda_l > 0.776 \end{cases} \tag{6}$$

where λ_l is the slenderness factor for local buckling, $\lambda_l = \sqrt{P_{ne} / P_{crl}}$;

P_{crl} is the elastic local buckling load of the gross section or perforated section that can be determined using elastic buckling analyses.

Distortional buckling strength (P_{nd})

$$P_{nd} = \begin{cases} P_y & for\ \lambda_d \le 0.561 \\ \left[1 - 0.25\left(\frac{P_{crd}}{P_y}\right)^{0.6}\right]\left(\frac{P_{crd}}{P_y}\right)^{0.6} P_y & for\ \lambda_d > 0.561 \end{cases} \quad (7)$$

where λ_d is the slenderness factor for distortional buckling, $\lambda_d = \sqrt{P_y / P_{crd}}$;

P_{crd} is the elastic distortional buckling load of the gross section or perforated section that can be determined using elastic buckling analyses. For the perforated section, if $\lambda_d \le \lambda_{d2}$, where λ_{d2} is determined as in Eq. (10) then:

$$P_{nd} = \begin{cases} P_{ynet} & for\ \lambda_d \le \lambda_{dl} \\ P_{ynet} - \left(\frac{P_{ynet} - P_{d2}}{\lambda_{d2} - \lambda_{d1}}\right)\left(\lambda_d - \lambda_{d1}\right) & for\ \lambda_{d1} < \lambda_d \le \lambda_{d2} \end{cases} \quad (8)$$

P_{ynet} is the axial yield strengths of the net section;
λ_{d1}, λ_{d2} are the slenderness factors of distortional buckling;
P_{d2} is the nominal axial strength of distortional buckling at λ_{d2};

$$\lambda_{d1} = 0.561\left(\frac{P_{ynet}}{P_y}\right) \quad (9)$$

$$\lambda_{d2} = 0.561\left[14\left(\frac{P_y}{P_{ynet}}\right)^{0.4} - 13\right] \quad (10)$$

$$P_{d2} = \left[1 - 0.25\left(\frac{1}{\lambda_{d2}}\right)^{1.2}\right]\left(\frac{1}{\lambda_{d2}}\right)^{1.2} P_y \quad (11)$$

2.2 Member in Flexure

The nominal moment of a beam (M_n) is the least of three values including global buckling moment (M_{ne}), local buckling moment (M_{nl}), and distortional buckling moment (M_{nd})

Global buckling moment (M_{ne})

$$M_{ne} = M_y \qquad \text{if } M_{cre} \ge 2.78M_y \quad (12)$$

$$M_{ne} = \frac{10}{9}\left(1 - \frac{10M_y}{36M_{cre}}\right)M_y \qquad \text{if } 0.56F_y < M_{cre} < 2.78\,M_y \tag{13}$$

$$M_{ne} = M_{cre} \qquad \text{if } M_{cre} \le 0.56M_y \tag{14}$$

where M_y is the yield moment of the gross sections; M_{cre} is the elastic global buckling moment that can be determined as follows:

$$M_{cre} = \frac{\pi}{K_y L}\sqrt{EI_y\left(GJ + \frac{\pi^2 EC_w}{(K_t L)^2}\right)}$$

The sectional properties are defined and determined as presented in Section 2.1 for the gross section and the perforated section.

Local buckling moment (M_{nl})

$$M_{nl} = \begin{cases} M_{ne} & for\ \lambda_l \le 0.776 \\ \left[1 - 0.15\left(\frac{M_{crl}}{M_{ne}}\right)^{0.4}\right]\left(\frac{M_{crl}}{M_{ne}}\right)^{0.4} M_y & for\ \lambda_l > 0.776 \end{cases} \tag{15}$$

where λ_l is the slenderness factor for local buckling, $\lambda_l = \sqrt{M_{ne}/M_{crl}}$;

M_{crl} is the elastic local buckling moment of the gross section or perforated section that can be determined using elastic buckling analyses.

Distortional buckling moment (M_{nd})

$$M_{nd} = \begin{cases} M_y & for\ \lambda_d \le 0.673 \\ \left[1 - 0.22\left(\frac{M_{crd}}{M_y}\right)^{0.5}\right]\left(\frac{M_{crd}}{M_y}\right)^{0.5} M_y & for\ \lambda_d > 0.673 \end{cases} \tag{16}$$

where λ_d is the slenderness factor for distortional buckling, $\lambda_d = \sqrt{M_y/M_{crd}}$;

M_{crd} is the elastic distortional buckling moment of the gross section or perforated section that can be determined using elastic buckling analyses. For the perforated section, if $\lambda_d \le \lambda_{d2}$, where λ_{d2} is determined as in Eq. (19) then:

$$M_{nd} = \begin{cases} M_{ynet} & for\ \lambda_d \le \lambda_{d1} \\ M_{ynet} - \left(\frac{M_{ynet} - M_{d2}}{\lambda_{d2} - \lambda_{d1}}\right)(\lambda_d - \lambda_{d1}) & for\ \lambda_{d1} < \lambda_d \le \lambda_{d2} \end{cases} \tag{17}$$

M_{ynet} is the yield moment of the net section;
λ_{d1} and λ_{d2} are the slenderness factors of distortional buckling;
M_{d2} is the nominal moment of distortional buckling at λ_{d2};

$$\lambda_{d1} = 0.673\left(\frac{M_{ynet}}{M_y}\right)^3 \tag{18}$$

$$\lambda_{d2} = 0.673\left[1.7\left(\frac{M_y}{M_{ynet}}\right)^{2.7} - 0.7\right] \tag{19}$$

$$M_{d2} = \left[1 - 0.22\left(\frac{1}{\lambda_{d2}}\right)\right]\left(\frac{1}{\lambda_{d2}}\right)M_y \tag{20}$$

3 Elastic Buckling Analyses for Cold-formed Steel Channel Members with Perforations

Elastic buckling analysis is a compulsory step to apply the DSM in the determination of capacities of cold-formed steel members. Section C20015 taken from the commercial sections is selected for the investigation, as illustrated in Fig. 1, where "C" indicates the channel section; the nominal dimensions include the depth D = 203 mm, the width B = 76 mm, the lip length L = 19.5 mm, and the thickness t = 1.5 mm. Rectangular hole shape is considered in this investigation with the hole heights varying from 0.2 to 0.8 times of the sectional depth (D), and the hole lengths varying from 0.5 to 2.0 times of the depth (D).

3.1 Elastic Sectional Buckling Analyses

The elastic sectional buckling analyses are carried out with the support of the module software program CUFSM [18]. This program requires simple input and directly provides output results including the local buckling and distortional buckling loads of both gross-section and perforated sections, as illustrated in Fig. 2. It was found that elastic local buckling loads only depend on the hole heights whereas they are hole lengths for distortional buckling loads [10]. The material properties regulated in the American Specification [3] include the strength F_y = 345 MPa, and Young's modulus E = 203400 MPa. The elastic buckling loads, therefore, are determined and reported in Table 1.

Table 1 shows that the elastic loads are seen as an increasing trend for local buckling modes, and the opposite trend is obtained for distortional buckling modes when the hole sizes increase. The distortional buckling loads of perforated sections are always less than those of the gross section. Meanwhile, the local buckling loads of the net section are even higher than those of this gross section (see the hole heights of 0.5D and 0.8D for compression, or 0.8D for bending). This means that local buckling modes will occur at the net section for small hole heights and at the gross section areas between holes for large hole heights. The reason for this has been explained in previous studies [19]. Therefore, the elastic local buckling loads (P_{crl}, M_{crl}) of the perforated sections can be taken as the smaller of these load values of the gross section and the net section for the design.

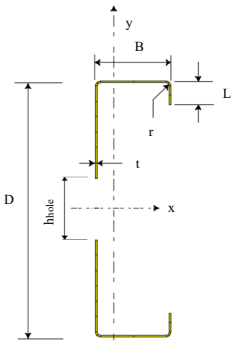

Fig. 1. Nomenclature

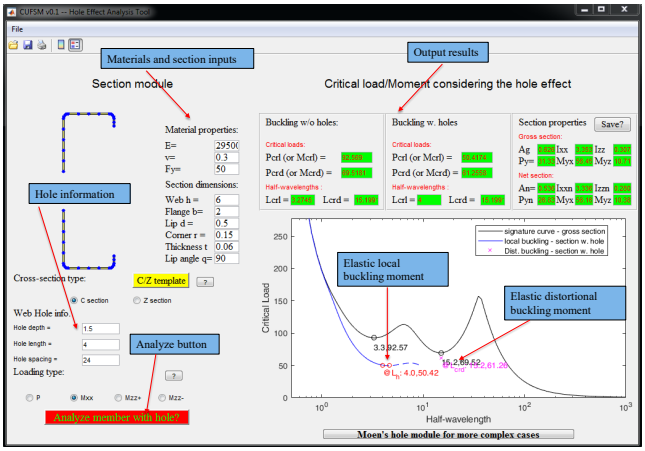

Fig. 2. The CUFSM software program

Table 1. Elastic buckling loads of C20015 section

Hole dimensions		Local buckling		Distortional buckling	
		Compression (kN)	Flexure (kNm)	Compression (kN)	Flexure (kNm)
No hole		33.01	10.49	76.67	10.31
h_{hole}	0.2D	31.93	5.65		
	0.5D	66.47	8.01		
	0.8D	114	10.98		
L_{hole}	0.5D			71.55	9.71
	D			66.29	9.04
	1.5D			60.85	8.32
	2D			55.18	7.53

3.2 Global Buckling Analyses

The C20015 section is chosen for the investigation with the length of 2500 mm. There are 05 symmetrical and even holes in the web of the investigated section as shown in Fig. 3. The variations of hole sizes have been presented above.

The specimen will be investigated under compression and bending. For compression, two different boundary conditions are applied to obtain two different global buckling modes. The first configuration allows the specimen to freely rotate about the strong axis (x-x) to obtain the flexural-torsional buckling mode (see Fig. 4) whereas the free rotation is for the weak axis (y-y) in the second configuration to get the flexural buckling mode (see Fig. 5). Warping displacements are restrained at two ends for both two configurations. The effective lengths, therefore, can be taken as follows: $L_x = L$, $L_y = L_z = 0.5L$ for the first configuration; $L_y = 0.5\ L$, $L_x = L_z = 0.5L$ for the

second configuration, where L is the specimen length. For bending, the specimen can freely rotate about both the strong axis (x-x) and the weak axis (y-y), and free warping displacements are applied at two ends as illustrated in Fig. 6. The effective lengths in all axes are equal to the specimen length (L). The elastic global buckling loads are determined as presented in Section 2 and are given in Table 2.

Table 2 shows that the buckling loads of flexural-torsional buckling modes under compression are the most significant impacts due to the appearance of web holes with the 50% capacity reduction compared to those of the gross section specimen, whereas they are about 30% reduction for the other buckling modes.

Both elastic sectional and global buckling loads calculated in this section will be used for the determination of the capacities of the investigated specimen with perforations in Section 4.

Table 2. Elastic global buckling loads of the C20015 specimen under compression or bending

h_{hole}/D	L_{hole}/D	Compression (kN)				Bending (kNm)	
		F-T	Δ%	F	Δ%	F-T	Δ%
0	0	389.32	100%	137.98	100%	12.61	100%
0.2	0.5	370.2	95.09%	136.06	98.61%	12.27	97.30%
	1	364.04	93.51%	134.15	97.22%	12.18	96.59%
	1.5	357.89	91.93%	132.24	95.84%	12.09	95.88%
	2	351.75	90.35%	130.32	94.45%	12	95.16%
0.5	0.5	329.13	84.54%	132.16	95.78%	11.49	91.12%
	1	314.06	80.67%	126.35	91.57%	11.23	89.06%
	1.5	299.21	76.85%	120.53	87.35%	10.96	86.92%
	2	284.53	73.08%	114.71	83.14%	10.68	84.69%
0.8	0.5	266.49	68.45%	126.11	91.40%	10.19	80.81%
	1	244.78	62.87%	114.24	82.79%	9.68	76.76%
	1.5	224.18	57.58%	102.36	74.18%	9.15	72.56%
	2	204.46	52.52%	90.49	65.58%	8.59	68.12%

Note: F, F-T stand for flexural and flexural-torsional buckling modes; Δ% stands for the deviations between the elastic global buckling loads of the perforated section members and the gross section members.

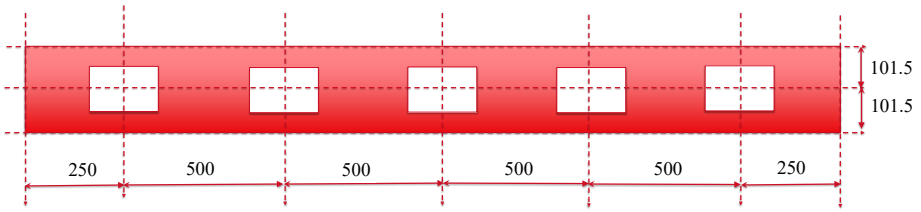

Fig. 3. The CUFSM software program

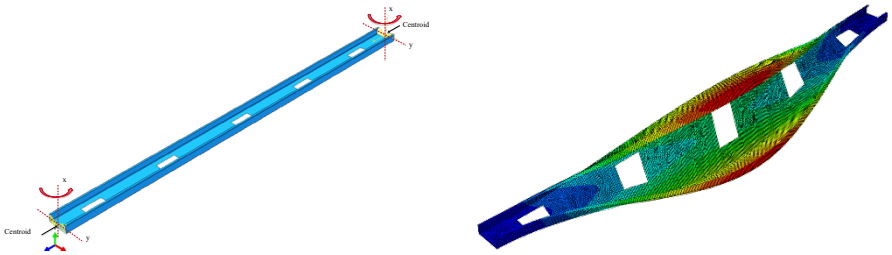

Fig. 4. The first configuration for compression and flexural-torsional buckling mode

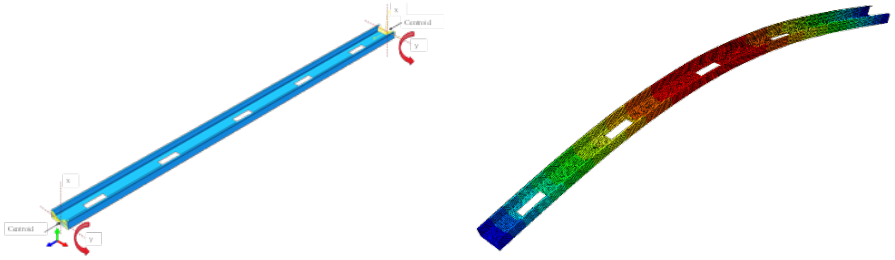

Fig. 5. The second configuration for compression and flexural buckling mode

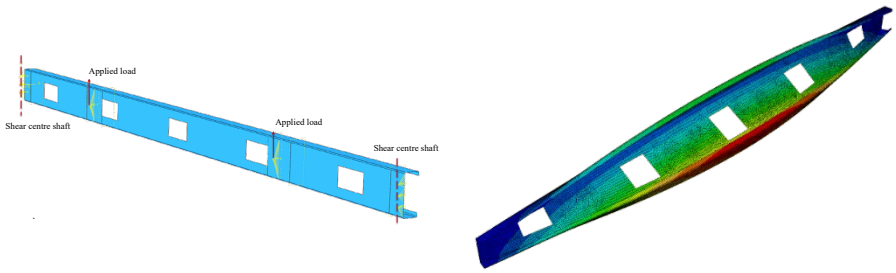

Fig. 6. The configuration for bending and flexural-torsional buckling mode

4 Investigation of Capacities of Cold-formed Steel Channel Members with Perforations under Compression or Bending

The obtained elastic buckling loads in Section 3 are used to directly determine the capacities of C20015 specimen with its length of 2500 mm and the variation of end boundary conditions by applying the Direct Strength Method design as presented in Section 2. There are three component strength values including global buckling strengths (P_{ne}, M_{ne}), local buckling strengths (P_{nl}, M_{nl}), and distortional buckling strengths (P_{nd}, M_{nd}) as listed in Tables 3, 4 and 5, respectively. The member capacities

of the investigated specimens are the least of the above strength values as given in Table 6 and illustrated in Fig. 7.

In terms of global buckling strengths (see Table 3), the effects of web holes are insignificant with less than 5% reductions for small hole heights of 0.2D in comparison with those of the gross section members, but they become noticeable with more than 20% reductions for large hole heights of 0.8D.

Table 3. Global buckling strengths of the C20015 specimen under compression or bending

Configurations	Hole dimensions		L_{hole}			
			0.5D	D	1.5D	2D
Config. 1 under compression (kN)	No holes		158.200			
	h_{hole}	0.2D	156.712	156.128	155.526	154.905
		0.5D	152.449	150.641	148.706	146.623
		0.8D	143.797	139.935	135.703	131.009
Config. 2 under compression (kN)	No holes		108.037			
	h_{hole}	0.2D	107.139	106.224	105.291	104.339
		0.5D	105.253	102.296	99.148	95.793
		0.8D	102.171	95.509	87.897	79.147
Bending (kNm)	No holes		9.831			
	h_{hole}	0.2D	9.728	9.699	9.670	9.640
		0.5D	9.465	9.367	9.262	9.149
		0.8D	8.935	8.689	8.403	8.063

Table 4. Local buckling strengths of the C20015 specimen under compression or bending

Configurations	Hole dimensions		L_{hole}			
			0.5D	D	1.5D	2D
Config. 1 under compression (kN)	No holes		77.732			
	h_{hole}	0.2D	76.352	76.171	75.985	75.792
		0.5D	75.924	75.351	74.734	74.067
		0.8D	73.155	71.898	70.505	68.941
Config. 2 under compression (kN)	No holes		60.945			
	h_{hole}	0.2D	59.914	59.586	59.250	58.906
		0.5D	59.932	58.846	57.676	56.413
		0.8D	58.801	56.306	53.372	49.875
Bending (kNm)	No holes		8.525			
	h_{hole}	0.2D	6.883	6.870	6.856	6.842
		0.5D	7.611	7.559	7.502	7.441
		0.8D	8.122	7.970	7.791	7.575

Table 5. Distortional buckling strengths of the C20015 specimen under compression or bending

Configurations	Hole dimensions		L_{hole}			
			0.5D	D	1.5D	2D
Config. 1 under compression (kN)	No holes		95.098			
	h_{hole}	0.2D	92.321	88.815	85.003	80.805
		0.5D	92.321	88.815	85.003	80.805
		0.8D	80.304	78.738	76.909	74.723
Config. 2 under compression (kN)	No holes		95.098			
	h_{hole}	0.2D	92.321	88.815	85.003	80.805
		0.5D	92.321	88.815	85.003	80.805
		0.8D	80.304	78.738	76.909	74.723
Bending (kNm)	No holes		8.908			
	h_{hole}	0.2D	8.768	8.533	8.263	7.946
		0.5D	8.768	8.533	8.263	7.946
		0.8D	8.430	8.309	8.162	7.946

Table 6. Member buckling strengths of the C20015 specimen under compression or bending

Configurations	Hole dimensions		L_{hole}			
			0.5D	D	1.5D	2D
Config. 1 under compression (kN)	No holes		77.732			
	h_{hole}	0.2D	76.352	76.171	75.985	75.792
		0.5D	75.924	75.351	74.734	74.067
		0.8D	73.155	71.898	70.505	68.941
Config. 2 under compression (kN)	No holes		60.945			
	h_{hole}	0.2D	59.914	59.586	59.250	58.906
		0.5D	59.932	58.846	57.676	56.413
		0.8D	58.801	56.306	53.372	49.875
Bending (kNm)	No holes		8.525			
	h_{hole}	0.2D	6.883	6.870	6.856	6.842
		0.5D	7.611	7.559	7.502	7.441
		0.8D	8.122	7.970	7.791	7.575

In terms of distortional buckling strengths (see Table 5), the hole impacts are unchanged for the hole heights of 0.2D and 0.5D, and have minor changes for the hole heights of 0.8D, whereas the effects of hole lengths become noticeable. The reductions of distortional buckling strengths are about 20% for compression and about 10% for bending in comparison with those of gross section members.

In terms of member capacities, it is found that the member failure modes are governed by local buckling modes for both cases due to the small thickness of the investigated specimen (see Tables 3 and 6). For compression, they are seen as downward trends for both two configurations if the hole dimensions increase. The capacity reductions are insignificant for small and intermediate hole heights (h_{hole} = 0.2D and

0.5D), but they are significant for large hole heights (h_{hole} = 0.8D), especially in the second configuration. For bending, it is found that the impacts of hole lengths are negligible, as seen in the minor deviations of member capacities with the variation of hole lengths. The novel point herein is the member capacities become higher for larger hole heights as seen in Fig. 7(c). As seen in Table 1 for sectional buckling analyses, the local buckling moments of net sections are less than those of the gross section, which means that local buckling modes governed the member failures occurring at the net sections. Therefore, the member capacities are seen as an upward trend with the increase in the hole heights due to the increasing trend of elastic local buckling moments as discussed in Section 3.

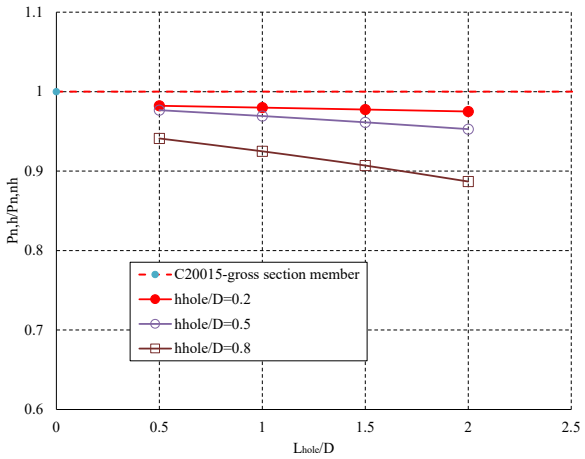

a) Configuration 1 for compression with flexural- torsional buckling modes

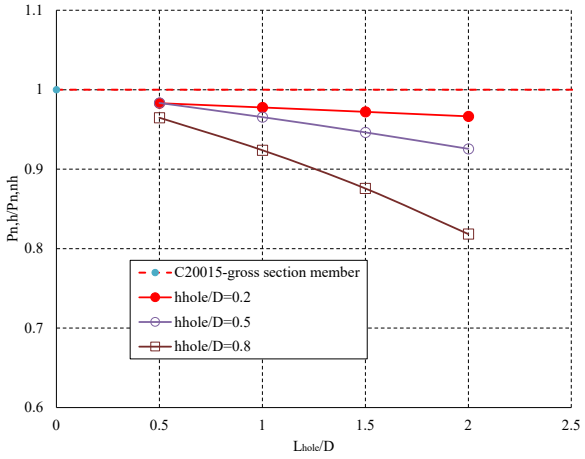

b) Configuration 2 for compression with flexural buckling modes.

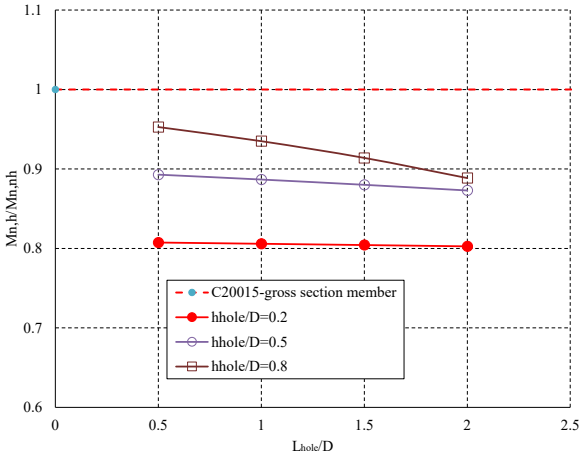

c) Bending configuration with flexural-torsional buckling modes.

Fig. 7. The capacities of C20015 section members

5 Conclusions

The paper investigated the effects of web hole dimensions on the capacities of cold-formed steel channel members under compression or bending. Variations of boundary conditions were used for the investigation to obtain different global buckling modes. The Direct Strength Method applied for the investigation was regulated in the American specification AISI S100-16. The CUFSM software program was used to support the elastic buckling analyses of the investigated section. The obtained strengths were the base for the analysis of the member behaviors. The several remarks are given as follows:

1) For global buckling strengths, the impacts of web holes are negligible for small hole heights, but become significant for large hole heights.

2) For distortional buckling strengths, the influence of web holes remains unchanged for hole heights of 0.2D and 0.5D, and has minor changes for hole heights of 0.8D compared to those of the rest of hole heights, whereas the impacts of hole lengths are found to be more significant.

3) Member buckling failures are governed by local buckling modes due to the small thickness of the investigated section.

4) For member buckling strengths, the compressive capacities undergo decreasing trend if the hole sizes increase, whereas the flexural capacities are found to significantly increase with the increase in the hole heights although they have negligible reductions due to the effects of hole lengths.

These remarks provide the base understanding of the behavior and strength of cold-formed steel channel members due to the effects of the web holes.

References

1. Yu, W.W., Laboube, R.A., Chen, H.: Cold-formed Steel Design. John Wiley and Sons. (2020).
2. Hancock, G.J., Pham, C.H.: New section shapes using high-strength steels in cold-formed steel structures in Austra.lia. Elsevier Ltd (2016).
3. American Iron and Steel Institute: North American Specification for the Design of Cold-Formed Steel Structural Members (2016).
4. AS/NZS 4600-2018: Australian / New Zealand Standard - Cold-formed steel structures. The Council of Standards Australia (2018).
5. Schafer, B.W., Peköz, T.: Direct Strength Prediction of Cold-Formed Members Using Numerical Elastic Buckling Solutions. In: Fourteenth International Specialty Conference on Cold-Formed Steel Structures (1998).
6. Li, Z., Schafer, B.W.: Buckling analysis of cold-formed steel members with general boundary conditions using CUFSM: Conventional and constrained finite strip methods. In: Twentieth International Specialty Conference on Cold-Formed Steel Structures. Saint Louis, Missouri, USA (2010).
7. Nguyen, V.V., Hancock, G.J., Pham, C.H.: Development of the Thin-Wall-2 for Buckling Analysis of Thin-Walled Sections Under Generalised Loading. In: Proceeding of 8th International Conference on Advances in Steel Structures (2015).
8. Pham, N.H.: Investigation of Sectional Capacities of Cold-Formed Steel SupaCee Sections. In: Proceedings of the 8th International Conference on Civil Engineering. ICCE 2021. Springer Singapore, vol. 213, pp. 82-94 (2022).
9. Pham, N.H., Vu, Q.A.: Effects of stiffeners on the capacities of cold-formed steel channel members. Steel Construction, vol. 14(4), pp. 270–278 (2021).
10. Moen, C.D., Schafer, B.W.: Elastic buckling of cold-formed steel columns and beams with holes. Engineering Structures. vol. 31(12), pp. 2812–2824 (2009).
11. Moen, C.D.: Direct Strength design for cold-formed steel members with perforations. PhD thesis. Johns Hopkins University. Baltimore (2008).
12. Moen, C.D., Schafer, B.W.: Experiments on cold-formed steel columns with holes. Thin-Walled Structures. vol. 46(10), pp. 1164–1182 (2008).
13. Moen, C.D., Schafer, B.W.: Impact of holes on the elastic buckling of cold- formed steel columns. In: International Specialty Conference on Cold-Formed Steel Structures. pp. 269–283 (2006).
14. Moen, C.D., Schafer, B.W.: Extending direct strength design to cold-formed steel beams with holes. In: 20th International Specialty Conference on Cold-Formed Steel Structures - Recent Research and Developments in Cold-Formed Steel Design and Construction. pp. 171–183 (2010).
15. Cai, J., Moen, C.D.: Elastic buckling analysis of thin-walled structural members with rectangular holes using generalized beam theory. Thin-Walled Structures. vol.107, pp. 274–286 (2016).
16. Moen, C.D., Schafer, B.W.: Elastic buckling of thin plates with holes in compression or bending. Thin-Walled Structures. vol. 47(12), pp. 1597–1607 (2009).
17. American Iron and Steel Institute: Development of CUFSM Hole Module and Design Tables for the Cold-formed Steel Cross-sections with Typical Web Holes in AISI D100. Research report. RP21-01 (2021).
18. American Iron and Steel Institute: Development of CUFSM Hole Module and Design Tables for the Cold-formed Steel Cross-sections with Typical Web Holes in AISI D100. Research report. RP21-02 (2021).

19. Pham, N.H.: Elastic Buckling Loads of Cold-Formed Steel Channel Sections with Perforations. Civil Engineering Research Journal. vol. 13(1), p.9 (2022).